J. Electroanal. Chem., 181 (1984) 245–266
Elsevier Sequoia S.A., Lausanne – Printed in The Netherlands

THE KINETICS OF THE REDUCTION OF PROTONS AT POLYCRYSTALLINE AND MONOCRYSTALLINE GOLD ELECTRODES

G.J. BRUG, M. SLUYTERS-REHBACH and J.H. SLUYTERS *
Van 't Hoff Laboratory of Physical and Colloid Chemistry, Padualaan 8, 3584 CH Utrecht (The Netherlands)

A. HAMELIN
Laboratoire d'Electrochimie Interfaciale du C.N.R.S., 1 Place A. Briand, 92190 Meudon (France)

(Received 3rd May 1983; in final form 10th July 1984)

ABSTRACT

The reduction of H^+ from 1 *M* $HClO_4$ and 1 *M* $NaClO_4$ solutions at polycrystalline and single crystal faces of very pure gold electrodes is studied by determining the forward rate constant k_f as a function of potential and of H^+ concentration. The techniques applied are dc current and impedance measurements both with a step-wise variation of dc potential (duration 4 s), and dc current measurements with a continuous potential variation. The consistency of the results is extensively tested and found to be quite satisfactory. Plots of ln k_f vs. potential are curved and exhibit limiting slopes corresponding to values for the operational transfer coefficient $\alpha = 1$ at positive and $\alpha = 0.5$ at negative potentials. This behaviour is discussed in terms of mechanistic models described in the literature and also an alternative mechanism is tentatively proposed. An increase in the rate constants is observed when the purity of the gold is less. The slight differences in the rate constants observed at single crystal faces of the same purity but with different crystallographic orientation are discussed.

(I) INTRODUCTION

The study of electrochemical kinetics at solid electrodes has often suffered from the poor quality of experimental results. As compared to the use of the dropping mercury electrode as a working electrode, the problems arising with solid electrodes became painfully clear and practically all of the meaningful data and theories on electrode kinetics were obtained and tested at the dropping mercury electrode.

This is even more true in double-layer studies and it is only recently that surface preparation techniques have been developed that allow precise and reproducible results to be obtained in this field [1–3]. However, just a reproducible state is still unsatisfactory if this state is not known down to the atomic level and if this state depends too strongly on the kind of preparation procedure. If the latter arises the

* To whom correspondence should be addressed.

0022-0728/84/$03.00

experiments are being made on an electrode in a well-defined though arbitrary state. The effect of various pretreatments on the cyclic voltammogram of a platinum electrode in 1 *M* H_2SO_4 has been demonstrated by Breiter [4], and further pioneering work on the best way to remove trace impurities from the surface was done by Gilman [5]. From these and many other works the conclusion is justified that anodic polarization just before the actual measurement brings about the desired removal of (adsorbed) impurities. The above-mentioned preparation procedures of gold electrodes [2,3] involve such a positive voltage perturbation, viz a slow sweeping to a well-chosen positive potential and back to the potential of interest. During this sweep the gold is superficially oxidized and then subsequently reduced.

The reasons for the excellent quality of the dropping mercury electrode are twofold: (a) the surface is smooth and clean and (b) mass transport by diffusion and convection is well-defined if the measurements are taken at a fixed time, say 4 s after drop birth. At solid electrodes it appears that the first property can be met to a reasonable extent by the preparation procedures now available [1–3] and the second by choosing a voltage–time relation starting from outside the faradaic region, thus allowing the diffusion problem to be equally well defined. This can conveniently be combined with the anodic pretreatment, e.g. in a way as shown in Fig. 1. The mass transport in this case will be described by the theory of the well-known potential step method. If the potential is recurrently controlled following Fig. 1, then a gold electrode is made to function in a way that has a close similarity to a dropping mercury electrode or a static mercury drop electrode, with comparable insensitivity to impurities in the solution.

A measuring technique most suitable for studies of electrode kinetics is undoubtedly the ac impedance method, because it is quite sensitive for mechanistic details of a particular system and moreover theoretically accessible for complications involved therein. For example, adsorption of reactants or intermediates, which can be expected to occur more often at a solid electrode than at a mercury electrode, can

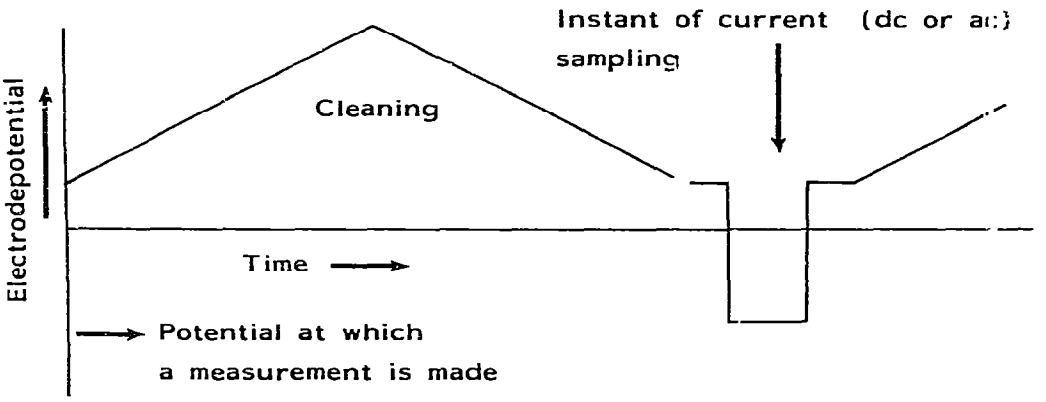

Fig. 1. Potential–time diagram of the programmed voltage perturbation.

be recognized unambiguously from the frequency spectrum of the interfacial admittance [6]. In addition, verification of the above stated expectations is most rigorously performed by inspecting the consistency of dc and ac results.

In this paper we report the results of a dc and ac study, applying the procedures advocated above to the reduction of H^+ ions at gold electrodes, both with polycrystalline and monocrystalline surfaces of different crystallographic orientations. This electrode reaction has been the subject of many previous studies. From a literature survey given by Kuhn and Byrne [7] and later articles of Sasaki and Matsuda [8] the impression is obtained that the kinetic parameters (the exchange current density and the transfer coefficient) depend strongly on the chemical state of the electrode surface, to such an extent that there is hardly any agreement between the results of different investigations. On the other hand, the proton reduction has been of theoretical interest for a long time as there is a number of classical treatments concerning the reaction mechanism as well as the dependence of the reaction rate on the nature of the electrode metal [9–13].

A question of particular interest is whether the kinetics of the H^+ reduction are, or should be, specifically dependent on the crystallographic orientation of a monocrystalline electrode [13–15]. Except for one publication [16], to our knowledge the effect of crystallographic orientation of gold electrodes has never been reported. We chose, therefore, to study the five faces of the face centered cubic system which should, according to the variation of the calculated surface free energy as a function of crystallographic orientation [17], show extreme behaviour, namely (111), (100), (110), (210) and (311). They were found to show extreme behaviour of the electrical double-layer as well [3].

Summarizing, the experiments to be described in this paper will be focussed on three topics: (i) reliability and consistency of data and interpretation, (ii) mechanistic considerations and (iii) (specific) effects of crystallographic orientation on mechanism and/or kinetic parameters.

(II) EXPERIMENTAL

(II.1) The solution

The solutions were prepared from twice distilled water and J.T. Baker Ultrex reagents. Sodium perchlorate solutions were prepared by adding perchloric acid to sodium carbonate in equivalent amounts. The cell solutions were either 1 *M* perchloric acid solutions or mixtures of perchloric acid and sodium perchlorate of 1 *M* total concentration.

The perchlorate anion was chosen because of its low tendency to adsorb specifically on the gold/water interface [18].

Oxygen was removed by purging with argon. The temperature of the cell solution was 25°C, unless stated otherwise.

(II.2) The electrodes

The single crystals were prepared from gold bars (Johnson–Matthey, 5 N) similarly to the Bridgeman method [2]. The crystals were grown from the melt in a graphite crucible, oriented with the aid of X-rays and cut along the desired crystallographic orientation.

The single crystal electrodes were mechanically polished with alumina of different grades down to 0.25 μm and the disturbed layer at the surface was eliminated by electrolytic dissolution and annealing [2].

The polycrystalline electrodes were mechanically polished with diamond paste (or with alumina) of different grades down to 0.25 μm.

Before each experiment the electrode was annealed in a highly oxygenated flame of methane gas and cooled by dipping into fresh twice distilled water. This was in order to avoid contact of the electrode with air [19]. In the cell the surface of the electrode was contacted with the surface of the solution following the dipping technique (pendant meniscus method) described by Dickertmann et al. [1]. All the calculations have been performed on the basis of the apparent geometric surface areas, which could be determined with an accuracy of ± 5 %.

The counter electrode was a gold sheet of 6 cm^2 (Johnson–Matthey, 5 N). All potentials were measured versus a saturated sodium chloride calomel electrode (SSCE). The counter electrode and the glassware were cleaned with aqua regia, thoroughly rinsed with twice distilled water and steamed.

(II.3) The measuring techniques

First the working electrodes were subjected to cyclic linear potential sweeps between -0.25 and ca. $+1.40$ V vs. SSCE with a sweep rate of 20 mV s^{-1} in order to obtain an indication of the purity and the physical state of the metal surface. This was done with 1 *M* $HClO_4$ as the cell solution. During each sweep the gold is superficially oxidized and subsequently reduced. The peaks in these cyclic voltammograms are characteristic for the structure of the interface. The application of these sweeps was continuously repeated until the cyclic voltammogram, by these characteristic peaks and its stationary behaviour, proved the interface to be in a reproducible state. At the start of each run of kinetic experiments the same procedure was applied, also as a check on the absence of impurities in the solution, or at the interface.

This slow change of the imposed potential for the anodic pretreatment was preferred to the fast potentiodynamic multipulse sequences employed by Gilman [5]. We feel that in our treatment irreversible changes of the outermost layer of atoms of the gold surface will be avoided and thus a possible effect of a changed physical state of the surface is eliminated or at least reduced.

For the dc measurements concerning the H^+ reduction two ways of varying the potential were applied:

(a) Potential sweeps into the faradaic region. The current flowing was recorded. The

value of this current was found to be independent of sweep rate between 20 and 5 mV s^{-1} which indicates that the current–voltage relation obtained is kinetically controlled.

(b) Potential steps from an initial potential of +0.400 V vs. SSCE, outside the faradaic region to subsequently more negative potentials in the faradaic region. In each step the current was sampled at 4 s after the start of it. In between two steps the potential was swept from the initial potential to a potential where the surface is oxidized (mostly +1.400 V vs. SSCE) and back in order to maintain a clean electrode. In this way quite reproducible current–voltage curves could be recorded.

All potential excursions were achieved with the aid of a digital to analog converter controlled by the HP 9830 calculator of the Network Analyser system described earlier [20].

For the ac measurements the same program of potential control as in the step method was applied. On this potential a sinusoidal ac voltage of 10 mV peak-to-peak was superimposed. The ac current amplitude and the phase angle were sampled 4 s after the start of the pulse with the Network Analyzer. The measurements were performed at twelve frequencies ranging from 80 Hz to 10 kHz and at 16 potentials.

Outside the faradaic region the double layer capacity was measured by the potential sweep method described by Clavilier [21] at a single frequency of 20 Hz. The values obtained provided another check of the state of the interfaces. With a good electrode the double layer capacitance values were found to be independent of the way of potential variation i.e. sweep or step.

(III) THEORY FOR DATA ANALYSIS

(III.1) The rate equation and the forward rate constant

It is generally accepted that the reduction of solvated protons to molecular hydrogen proceeds via a step-wise mechanism involving the following reactions: the discharge reaction

$$H^+(H_2O)_h + e^- \rightleftarrows h\,H_2O + H_{ad} \qquad (R1)$$

followed by either, or both, the ion + atom reaction

$$H^+(H_2O)_h + H_{ad} + e^- \rightleftarrows h\,H_2O + H_2 \qquad (R2)$$

and the combination reaction

$$2\,H_{ad} \rightleftarrows H_2 \qquad (R3)$$

So the intermediate is supposed to be adsorbed atomic hydrogen, which either reacts with a second proton or combines with another adsorbed hydrogen atom, to form molecular hydrogen at the surface. It is assumed that the hydrogen molecule desorbs very fast.

The implications of this mechanism, and especially of the strength of the adsorption of atomic hydrogen, for the current–voltage characteristic has been

treated in the literature several times [9,11–13,22,23]. A general rate equation accounting for R1, R2 and R3 simultaneously at any degree of coverage, is severely complex. It is usual therefore to consider several limiting cases separately, as for example in refs. 9, 12 and 13, assuming the symmetry factors of the three steps to be equal to 0.5. In the case of an irreversible reduction such a rate equation is of the type

$$-j_F = Fk_f c_{H^+}^{\nu_{H^+}} c_{H_2}^{\nu_{H_2}} \tag{1}$$

The potential dependence of k_f can be characterized by

$$(RT/F)\mathrm{d}(\ln k_f)/\mathrm{d}E = -\alpha \tag{2}$$

The asymptotic values of the cathodic transfer coefficient α and the stoichiometric coefficients depend on the type of mechanism, cf. the tabulations given in refs. 9 and 23.

(III.2) The dc current

For dc experiments, eqn. (1) will hold for the dc current $\bar{j}_F$ and the dc surface concentrations $\bar{c}_{H^+}$ and $\bar{c}_{H_2}$, the latter two being generally different from the bulk concentrations $c^*_{H^+}$ and $c^*_{H_2}$.

As we worked with solutions that were originally free from hydrogen, it is more convenient to eliminate $\bar{c}_{H_2}$. As a good approximation this can be done by introducing a linear relationship between $\bar{j}_F$ and $\bar{c}_{H_2}$, following the diffusion layer model:

$$-\bar{j}_F = 2\,Fa_{H_2}\bar{c}_{H_2} \tag{3}$$

with $a_{H_2} = D_{H_2}/\delta_{H_2}$, i.e. the diffusion coefficient of dissolved H_2 divided by the diffusion layer thickness. Equation (3) requires that no hydrogen gas evolves. If this relation is substituted in the dc version of eqn. (1) we obtain

$$-\bar{j}_F = Fk_f^{1/(1-\nu_{H_2})}(2a_{H_2})^{-\nu_{H_2}/(1-\nu_{H_2})}\bar{c}_{H^+}^{\nu_{H^+}/(1-\nu_{H_2})} \tag{4}$$

If $\nu_{H_2} \neq 0$ this has consequences for the apparent reaction order in $\bar{c}_{H^+}$ and the potential dependence of $\bar{j}_F$. For this reason we have tabulated in Table 1 the values of ν_{H^+}, ν_{H_2} and α for the limiting cases that are usually considered, together with values of the quantities

$$\nu'_{H^+} = (\partial \ln(-j_F)/\partial \bar{c}_{H^+})_E = \nu_{H^+}/(1-\nu_{H_2}) \tag{5a}$$

and

$$\alpha' = (RT/F)(\partial \ln(-j_F)/\partial E)_{\bar{c}_{H^+}} = \alpha/(1-\nu_{H_2}) \tag{5b}$$

The tabulated numbers have been deduced from general rate equations identical to those derived in ref. 13. It may be noted that a partly similar compilation in a paper of Conway and Salomon [23] probably contains a printing error as regards case C.

At high H^+ concentrations the effect of mass transfer on $\bar{c}_{H^+}$ will be negligible and it is allowable to replace $\bar{c}_{H^+}$ by $c^*_{H^+}$. Depending on the reaction mechanism

and the extent of adsorption of the hydrogen atom, the reaction order in $c^*_{H^+}$ can be second, first or zero order, but also in between these values according to the ν'_{H^+} values in Table 1.

At low H^+ concentrations the diffusion of H^+ should be accounted for and even if we apply a diffusion layer model:

$$-\bar{j}_F = Fa_{H^+}(c^*_{H^+} - \bar{c}_{H^+})$$

with $a_{H^+} = D_{H^+}/\delta_{H^+}$, this will lead to a complicated expression, unless the reaction order in c_{H^+} equals unity. If $\nu'_{H^+} = 1$, the rigorous solution of the semi-infinite linear diffusion problem can be employed. In that case we have [24]

$$-\bar{j}_F = Fc^*_{H^+}\lambda \exp(\lambda^2 t)\ \mathrm{erfc}(\lambda t^{1/2}) \tag{6}$$

with

$$\lambda = [k_f(E)]^{1/(1-\nu_{H_2})}(2a_{H_2})^{-\nu_{H_2}/(1-\nu_{H_2})}D_{H^+}^{-1/2} \tag{7}$$

Note that eqn. (7) reduces to the "normal" expression $\lambda = k_f(E)D_{H^+}^{-1/2}$ if $\nu_{H_2} = 0$, and that we have $\nu_{H_2} \neq 0$ only in the perhaps less probable cases Ab, Ac, Bb and Bc, see Table 1.

The treatment above of the dc current rests upon the assumption that the electrolysis time is sufficiently long to establish the stationary state, i.e. that the rate of reaction R1 equals the sum of the rates of R2 and R3.

TABLE 1

Stoichiometric coefficients and transfer coefficients for the relation $\bar{j}_F = f(E, \bar{c}_{H^+}, \bar{c}_{H_2})$, cf eqn. (1), and for the relation $\bar{j}_F = f(E, \bar{c}_{H^+})$ after elimination of $\bar{c}_{H_2}$ (see text). θ_H = fractional surface coverage of atomic hydrogen

Mechanism		ν_{H^+}	ν_{H_2}	α	ν'_{H^+}	α'
A. R1 + R2	(a) $\theta_H \ll 0.5$	1	0	0.5	1	0.5
R1 rate determining	(b) $\theta_H \approx 0.5$	1.5	−0.5	1	1	0.67
	(c) $\theta_H \gg 0.5$	2	−1	1.5	1	0.75
B. R1 + R3	(a) $\theta_H \ll 0.5$	1	0	0.5	1	0.5
R1 rate determining	(b) $\theta_H \approx 0.5$	1	−0.25	0.5	0.8	0.4
	(c) $\theta_H \gg 0.5$	1	−0.5	0.5	0.67	0.33
C. R1 + R2	(a) $\theta_H \ll 0.5$	2	0	1.5	2	1.5
R2 rate determining	(b) $\theta_H \approx 0.5$	1.5	0	1	1.5	1
	(c) $\theta_H \gg 0.5$	1	0	0.5	1	0.5
D. R1 + R3	(a) $\theta_H \ll 0.5$	2	0	2	2	2
R3 rate determining	(b) $\theta_H \approx 0.5$	1	0	1	1	1
	(c) $\theta_H \gg 0.5$	0	0	0	0	0

(III.3) The charge transfer resistance and the interfacial admittance

If the stationary state is assumed to hold also on the ac time scale, the charge transfer resistance, R_{ct}, defined as

$$R_{ct}^{-1} = (\partial j_F/\partial E)_{c_{H^+}, c_{H_2}} \tag{8}$$

is easily derived from eqn. (1) and (2). It follows that

$$R_{ct}^{-1} = [\mathrm{d}(\ln k_r)/\mathrm{d}E]\, j_F = -(F/RT)\alpha j_F \tag{9}$$

Because of the irreversible character of the H^+ reduction the absence of a mass transport impedance can safely be assumed, so that R_{ct}^{-1} will be the only element parallel to the double layer admittance. In a separate study [25] we have paid attention to the fact that at solid electrodes the latter should not be represented by a pure capacitance, but rather by the so-called "constant phase element" (CPE). It was shown that reliable R_{ct} values can be obtained using an extrapolation procedure followed by an internal check.

Since the ac time scale of impedance measurements—using frequencies up to several kHz—is much shorter than the dc time scale, non-stationary proceeding of the reaction sequence is not unlikely to be observed in the interfacial admittance. In that case the faradaic admittance Y_F becomes more complex, as has been shown by Gerischer and Mehl [10]. Following their derivation the frequency dependence of Y_F is expressed by [6,10]

$$Y_F = R_\infty^{-1} - \frac{ab}{b^2 + \omega^2 C_H^2} + i\frac{\omega C_H a}{b^2 + \omega^2 C_H^2} \tag{10}$$

where R_∞, a and b are functions of $\bar{c}_{H^+}$, the fractional surface coverage θ_H and E; $C_H = F\Gamma_m$ (Γ_m is maximum coverage) is called the "adsorption capacity". It can be shown that

$$R_{ct}^{-1} = R_\infty^{-1} - (a/b) \tag{11}$$

Evidently this is the low frequency limit of the real part of eqn. (10). Note, however, that a possible non-stationary behaviour can be reflected by the imaginary part, which reduces at low frequency to $i\omega C_H$, i.e. to an "adsorption capacitance" parallel to the double layer admittance.

At sufficiently high frequencies the second term in eqn. (10) will become infinitely small, so that apparently a "charge transfer resistance" R_∞ remains. The meaning of this parameter is, of course, different from that of R_{ct} and most probably its value will not be consistent with eqn. (9).

We may conclude that a combined analysis of ac and dc results can be useful for drawing conclusions about the mechanism of the overall H^+ reduction.

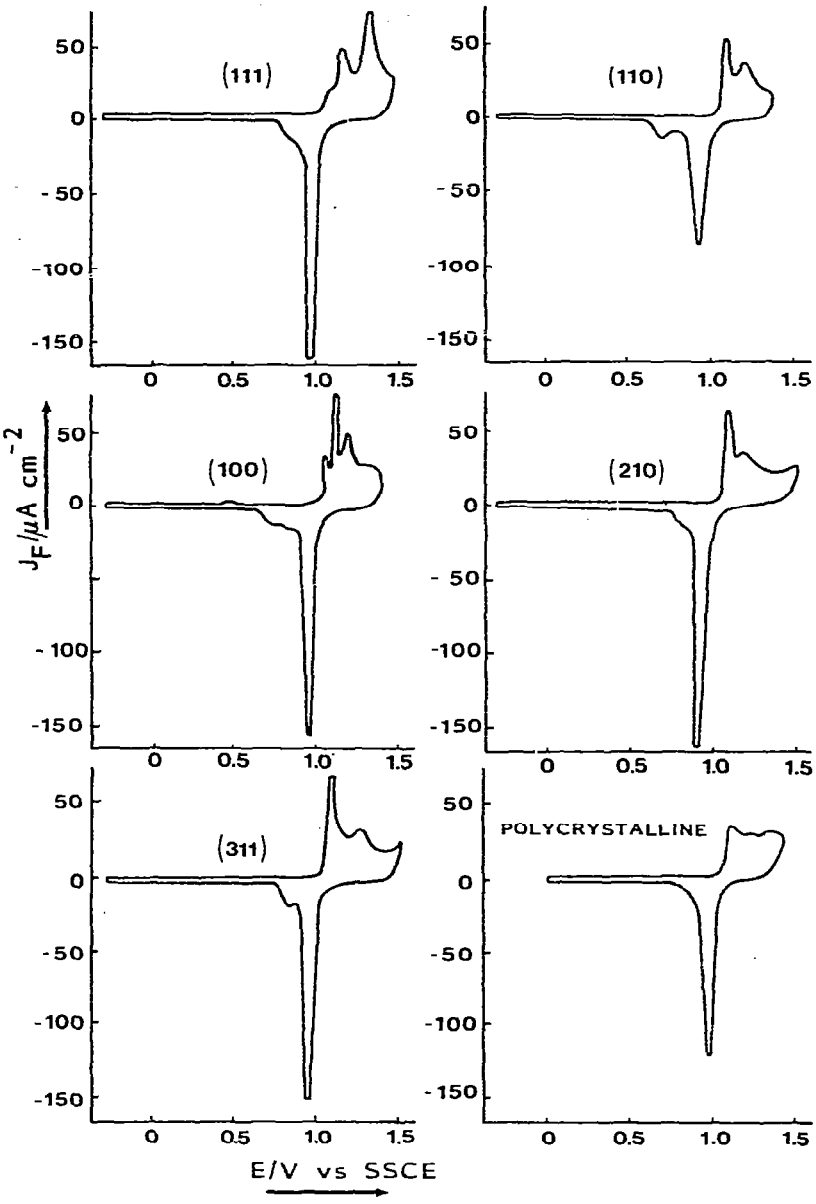

Fig. 2. Cyclic voltammograms for the five gold single crystal faces and polycrystalline gold in 1 *M* perchloric acid, sweep rate 20 mV s^{-1}.

(IV) RESULTS AND DISCUSSION

(IV.1) Characterization of the electrodes

(IV.1.1) Cyclic voltammograms

The cyclic voltammograms recorded in 1 *M* $HClO_4$ solution before each series of experiments are reproduced in Fig. 2. The applied potential region includes the double-layer region (−0.250 to ca. +0.6 V vs. SSCE) as well as the region of oxide formation (+0.6 V to +1.4 V vs. SSCE). The latter shows a fine structure that is significantly specific for the crystal orientation.

Some controversy exists in the literature about the question as to whether such fine structures are essentially related to different stages of oxide formation, or are rather due to trivial causes such as low surface roughness or edge effects. Discussions on this problem can be found, for example, in the works of Sotto [26] and of Dickertmann et al. [27]. For our purpose it was sufficient to use the cyclic voltammograms as a monitor for surface reproducibility, as we found the kinetics of H^+-reduction to be quite reproducible if the patterns in Fig. 2 were established. The potentials of the peaks observed are listed in Table 2. If, instead of argon, hydrogen was purged into the solution, no oxidation or adsorption of hydrogen was observed between −0.50 and +1.40 V vs. SSCE. In the cyclic voltammograms no signs of changes were observed during the experiments indicating that repeated cycling under our conditions does not affect the roughness of the electrode nor the structure of the top layer of atoms at the surface.

TABLE 2

Potentials of peaks in the cyclic voltammogram of single crystal faces of gold in 1 *M* perchloric acid. Sweep rate 20 mV s^{-1}; temperature 19±2°C

Crystallographic orientation	Potentials of oxidation peaks *E*/V vs. SSCE	Potentials of reduction peaks *E*/V vs. SSCE
(111)	1.07 (shoulder)	0.94
	1.13	0.82 (shoulder)
	1.29	
(110)	1.09	0.95
	1.21	0.70
(100)	0.48 (minor peak)	0.96
	1.06	0.82 (shoulder)
	1.10	0.73 (shoulder)
	1.18	
	1.32	
(210)	1.07	0.95
	1.18	0.81 (shoulder)
(311)	1.095	0.95
	1.28	0.845
		0.78 (shoulder)

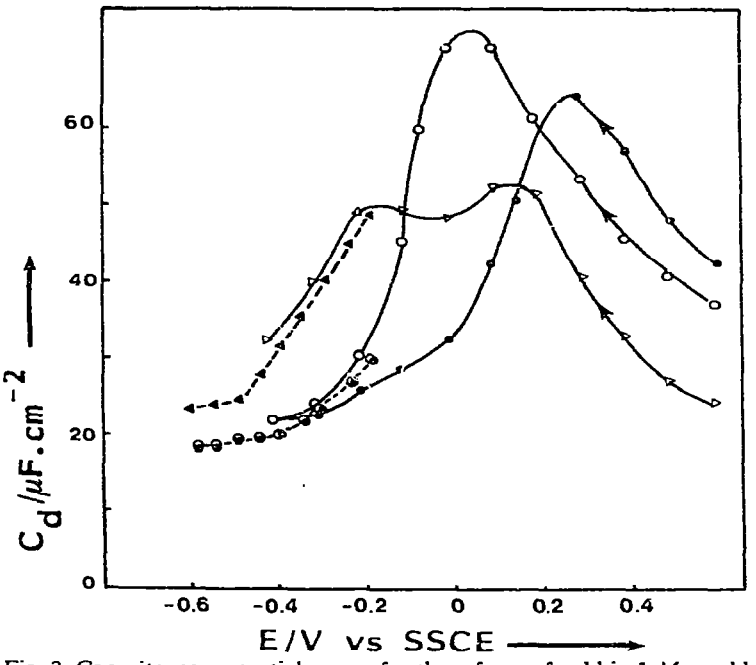

Fig. 3. Capacitance–potential curves for three faces of gold in 1 *M* perchloric acid obtained: by potential sweep (———), by potential step (— — —), (●) (111), (△) (110) and (○) (100).

(IV.1.2) Double-layer capacitance

In the non-faradaic region, i.e. at approximately $-0.40 < E < +0.60$ V vs. SSCE, the double layer capacitance C_d of three single crystal electrodes ((111), (110) and (100)) was measured at a single frequency, 20 Hz, by the potential sweep method described by Clavilier [21]. Within the faradaic region of H^+ reduction the values of C_d were obtained from the frequency spectrum analysis, as has been described elsewhere [25]. The results, represented in Fig. 3, reveal that the two sets connect reasonably well at each of the three single crystal electrodes. The capacitance in the faradaic region appears to have reached the well-known minimum (ca. 20 μF cm^{-2}) without any evidence of an adsorption capacitance being present.

(IV.2) H^+ reduction at a polycrystalline electrode; concentration dependence

In a first series of experiments dc step voltammograms were measured at the polycrystalline electrode in contact with 1 *M* $NaClO_4$ solution containing $HClO_4$ at concentrations ranging from 4.75×10^{-3} to 34×10^{-3} *M*. The limiting current density $j_{F,l}$ was found to be proportional to $c^*_{H^+}$. Using the Cottrell equation, the diffusion coefficient was calculated: $D_{H^+} = 77.4 \times 10^{-6}$ cm^2 s^{-1}, in very good agreement with the value 76.0×10^{-6} obtained from a dc polarogram at the dropping mercury electrode. The step voltammograms were normalized by plotting $j_F/j_{F,l}$ vs. E in Fig. 4. The coincidence of the data is satisfactory and gives evidence that eqn. (6) is applicable. Using this equation and assuming $\nu_{H_2} = 0$ the values of

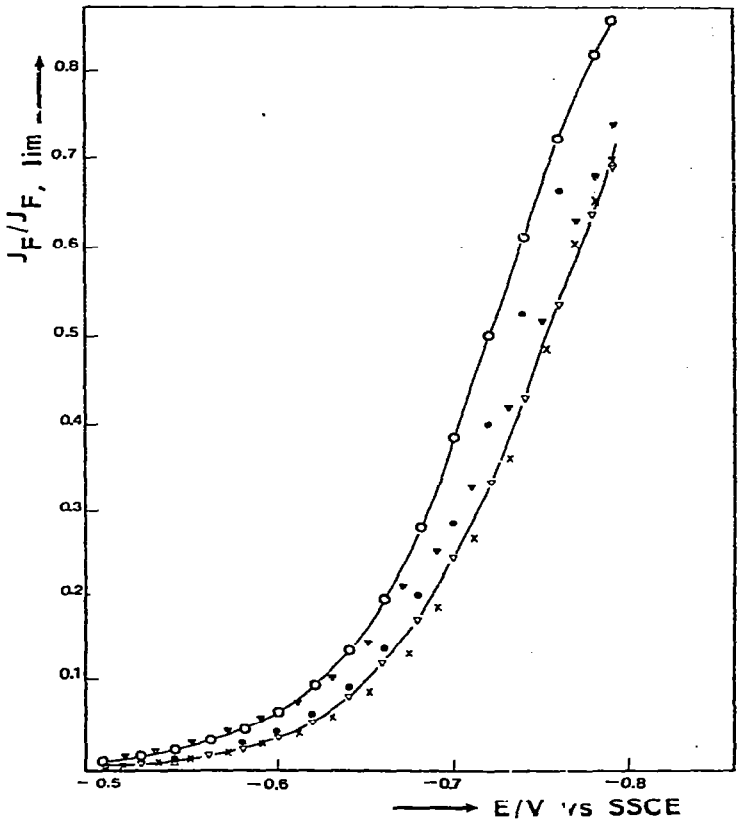

Fig. 4. Normalized potential step voltammograms at a polycrystalline gold electrode for different concentrations of solvated protons: (▽) 4.75×10^{-3} (○) 9.5×10^{-3}, (●) 10.5×10^{-3}, (×) 18.6×10^{-3}, (▼) 34×10^{-3} mol l^{-1}.

ln k_f were calculated, which are plotted against potential in Fig. 5, together with a part of the ln k_f vs. E plot obtained at the polycrystalline electrode in 1 M $HClO_4$.

Although there are some non-systematic discrepancies between the different runs, each run (except the one at 34 mM H^+) clearly produces an almost straight ln k_f vs. E plot, with a slope corresponding to a transfer coefficient ranging from $\alpha = 0.50 \pm 0.02$ in the most negative potential region to $\alpha = 0.60 \pm 0.02$ at more positive potentials. The mutual difference between the ln k_f values at fixed potential in Fig. 5 is 0.5 or less. This gives a good indication of the overall reproducibility of essentially different runs. Moreover, the rate constants determined for the 1 M $HClO_4$ solution connect very well to the results at low H^+ concentration. Especially the latter fact proves that in the potential range considered the reaction is first order in c_{H^+}.

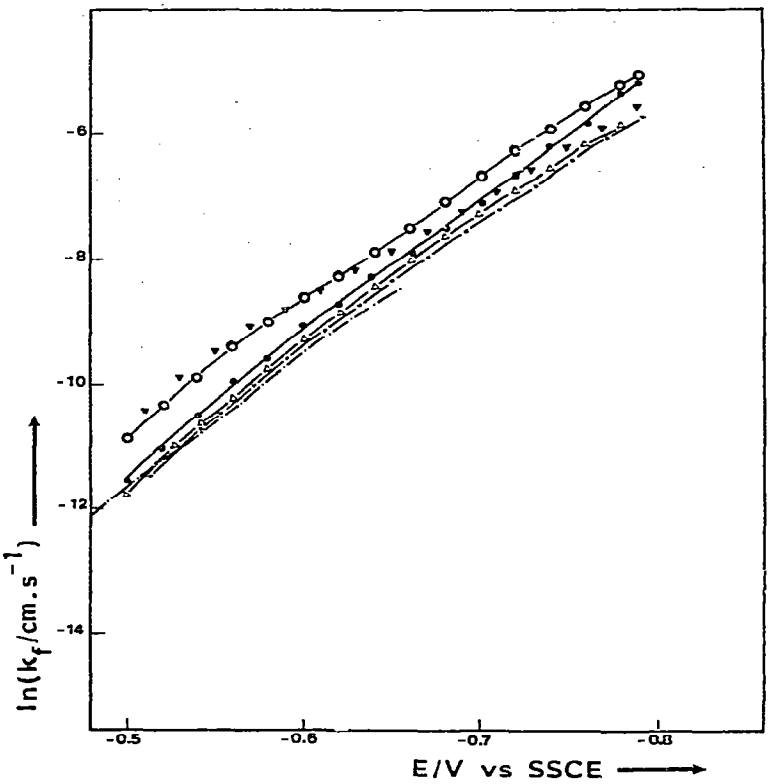

Fig. 5. The forward rate constant vs. potential derived from the data in Fig. 3. (△) 4.75×10^{-3}, (○) 9.5×10^{-3}, (●) 10.5×10^{-3}, (×) 18.6×10^{-3}, (▲) 34×10^{-3} and (-·-·-) 1.00 mol l^{-1}. $E^{\circ} = -0.235$ V vs. SSCE.

As in the next section the potential dependence of the reaction is studied in a more positive potential region (between -0.2< and -0.6 V vs. SSCE), a separate experiment was performed to determine the reaction order in c_{H^+} at potentials as high as possible. Since then the current densities are extremely low, a working electrode with a large surface area (ca. 10 cm^2, also 5 N quality) was used to measure dc step voltammograms of a solution containing 1 *M* $HClO_4$ and a solution containing 0.1 *M* $HClO_4 + 0.9$ *M* $NaClO_4$. The currents obtained yield a fairly straight Tafel plot in the region -0.23 to -0.34 V vs. SSCE for 1 *M* H^+ and in the region -0.28 to -0.38 V for 0.1 *M* H^+. The slopes of these Tafel plots correspond to $\alpha = 0.93 \pm 0.02$ in both cases. The reaction order in c_{H^+} calculated as $\Delta \log j_F/\Delta \log c_{H^+}$, varied from 0.96 at $F = -0.28$ V to 0.91 at $E = -0.38$ V vs. SSCE.

In may be noted that this behaviour is observed at potentials quite close to the standard potential of the H^+/H_2 reaction, which equals -0.235 V vs. SSCE.

(IV.3) H^+ reduction from 1 M $HClO_4$ at mono- and polycrystalline electrodes

(IV.3.1) Potential dependence

The impedance measurements were analyzed using the procedure developed in a separate paper [25] to obtain the value of the charge transfer resistance R_{ct} as a function of dc potential. In Fig. 6 plots are made of (a) $\ln(R_{ct}^{-1}/c^*_{H^+}) + \ln(RT/F^2)$, derived from the impedance measurements and (b) $\ln(j_F/Fc^*_{H^+})$, derived from the dc step voltammograms, both measured at the polycrystalline electrode and at three different single crystal electrodes in contact with a 1 M $HClO_4$ solution. Because of

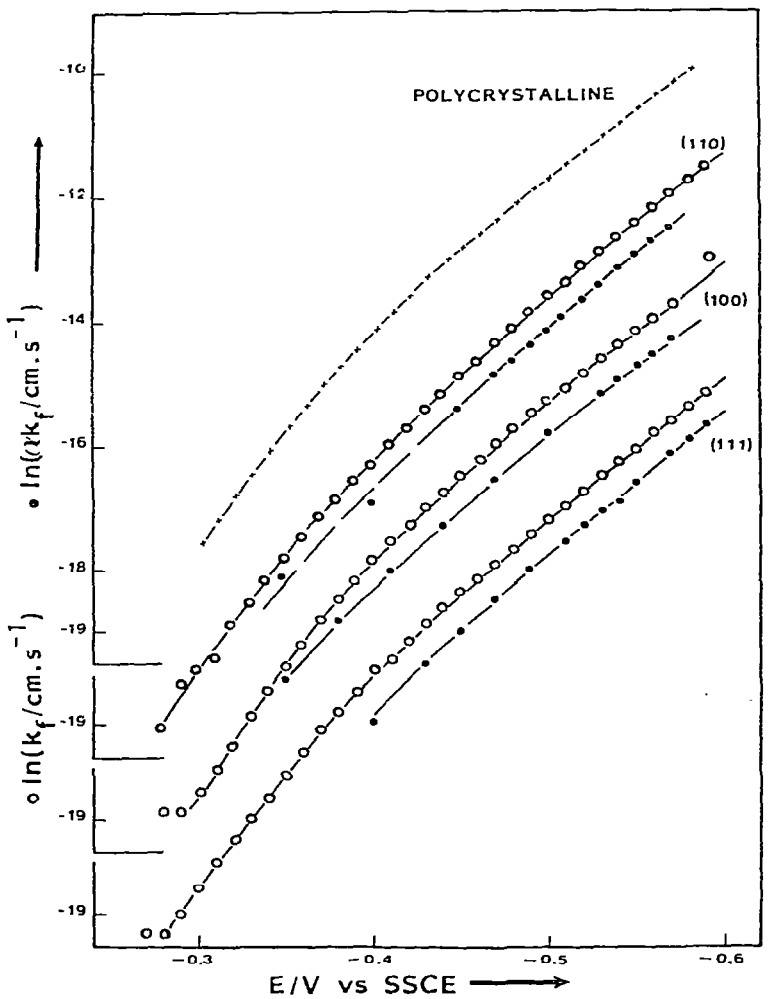

Fig. 6. $\ln(k_f)$ and $\ln(\alpha k_f)$ vs. potential obtained for single crystal faces of gold (100), (110) and (111) and polycrystalline gold (only $\ln k_f$) in 1 M perchloric acid from potential step (○) and impedance measurements (●) respectively.

the high H^+ concentration diffusion control will be negligible in the potential region investigated and so, if $\nu_{H_2} = 0$ and $\nu_{H^+} = 1$ curve (b) should represent $\ln k_f$ directly, whereas curve (a) will represent $\ln(\alpha k_f)$. It appears that the experimental data are fairly consistent with these premises corresponding to a value of $\alpha = 0.55$ to 0.6 at potentials between -0.60 and -0.45 V vs. SSCE, and to increasing α values at more positive potentials. A similar combined analysis of impedance and dc step data at a low H^+ concentration (6.4 mM) in 1 M $NaClO_4$ exhibited the same consistency and confirmed the slight change of α with potential ($\alpha = 0.47$ to 0.65) as mentioned above.

The reproducibility of these measurements in 1 M $HClO_4$ was tested several times by repeating the runs. In both the current and the impedance measurements any discrepancy never exceeded 2 %. Since the potential programming described in the experimental section causes one run to last about 4 h, it can be concluded that the reactivity of the electrode surface exposed to the solution remains stable. It can be inferred therefore that the electrode surface remains in the same chemical and physical state during its contact with the cell solution. The considerable effect of preanodization, as observed by Sasaki and Matsuda [8], is absent in our experiments. Combining our whole set of data (see also section IV.2), we find a gradual increase in α from the value 0.5 at $E = -0.75$ V vs. SSCE up to unity at $E = -0.24$ V vs. SSCE.

In addition to the step measurements also current–potential curves were recorded for five single crystal faces in 1 M $HClO_4$ by the potential sweep method described at several scan rates. These measurements were performed at room temperature, 19 ± 2°C. The resulting voltammograms appeared to be independent of scan rate if the scan rate was less than 20 mV s^{-1}. However, for the (100) face some dependence on scan rate remained down to 2.5 mV s^{-1}. The values of the rate constant, calculated as $\ln k_f = \ln(-j_F/Fc^*_{H^+})$, and plotted against potential in Fig. 7B, are quite close to the data obtained from the step measurements (Fig. 7A). However, the slopes of the $\ln k_f$ vs. E curves from the sweep experiments appear to be less steep, especially at the lower current densities. This tendency was found to be stronger at higher sweep rates: e.g. $\alpha = 0.53$ in the region -0.40 to -0.50 V vs. SSCE, as compared with $\alpha = 0.65$ obtained from the step experiments in this region.

In connection with this, it may be mentioned that both Kuhn and Byrne [7] and Sasaki and Matsuda [8] determined Tafel plots at a polycrystalline gold electrode of 4 N quality in H_2SO_4 solutions and found a much steeper Tafel slope at low current densities compared with our step experiments. Kuhn and Byrne mentioned that currents at the lowest polarization generally took 2 or 3 hours to become steady. On the other hand, Schmid [28] has studied a polycrystalline gold electrode in 1 M $HClO_4$ applying a procedure involving intermediate anodic prepolarizations and obtained a curved $\ln k_f$ vs. E plot with slopes quite close to the slopes in our Fig. 7A. This could suggest a conclusion that the electrolysis time and the treatment of the electrode between two measurements have an effect on the curvature of the Tafel plots.

Proton reduction from perchloric acid on single crystalline (111), (100) and (110)

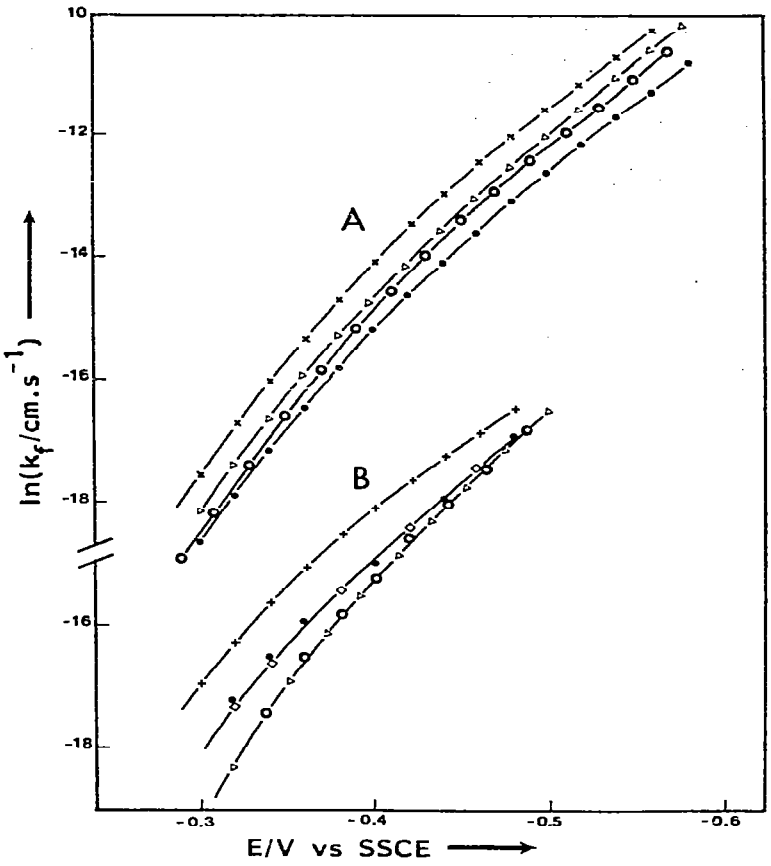

Fig. 7. $\ln(k_f)$ vs. potential for 1 *M* perchloric acid. (A) potential step measurements, (B) potential sweep measurements. (+) (311) 4 N, (□) (210) ≡ (311), (○) (100), (●) (111) and (△) (110); (×) polycrystalline electrode. $E^\circ = -0.235$ V vs. SSCE.

faces of gold has been studied by Bicelli and Graziano [16]. They also observed curved Tafel plots, though with rather varying and irreproducible values for the slopes.

In one experiment, also reproduced in Fig. 7B, a (311) crystal face electrode made of gold 4 N (instead of gold 5 N used in all the other experiments) was used. The rate constants at this electrode are systematically higher by an amount of $\ln k_f$ = ca. 1.0, which is certainly more than the experimental errors in k_f due to the surface roughness (ca. 1 to 7 %) and the inaccuracy in the determination of the geometric area (±5 %).

(IV.3.2) The mechanism of the proton reduction at gold

The curved plots in Fig. 7 can be very well described mathematically by an expression of the form

$$1/k_f = \exp(0.5\phi)/L_1 + \exp(\phi)/L_2 \qquad (12)$$

where $\phi = (F/RT)(E - E°)$. Values of L_1 and L_2 (as yet empirical quantities), calculated taking $E° = -0.235$ V vs. SSCE, are listed in Table 3. The fit to eqn. (12) is quite exclusive, i.e. attempts to replace $\exp(\phi)$ by e.g. $\exp(1.5\phi)$, gave no satisfactory fit. As eqn. (12) is obeyed by our results down to $\phi = 0$, it is easily realized that for any possible third term, e.g. $\exp(1.5\phi)/L_3$ or $\exp(2\phi)/L_3$, the value of L_3 should be larger than ca. 30 times L_2. It may be worth noting that the region of curvature in our Tafel plots is quite large (over 0.150 V), in contrast to the sharp transition from one slope to another often reported in literature [29].

We conclude that the term in $\exp(0.5\phi)$ represents the limiting behaviour of our results in the high overvoltage region (see also Fig. 5) and the term in $\exp(\phi)$ represents the limiting behaviour at potentials near $E°$, hence we may try to deduce a plausible choice of mechanism regarding the cases of limiting behaviour collected in Table 1. It is obvious that limiting behaviour with $\alpha = 1$ at positive E only occurs in mechanism C or D with $\theta_H \approx 0.5$. Then the limiting behaviour with $\alpha = 0.5$ at negative E can logically be explained by a change to either mechanism C with

TABLE 3

Coefficients of the two exponential terms in eqn. (17) and the corresponding limiting values of the operational transfer coefficient

	First term		Second term	
	$10^8 L_1$/cm s^{-1}	α_{lim}	$10^9 L_2$/cm s^{-1}	α_{lim}
A. Step measurements				
polycryst.	6.0	0.50	2.2	1.00
(110)	4.2	0.50	1.0	1.02
	3.4	0.52	1.1	1.02
(100)	3.5	0.50	0.75	1.02
(111)	1.8	0.52	0.8	1.00
B. Sweep measurements				
(110)	3.0	0.49	0.4	1.05
(100)	3.0	0.49	0.4	1.05
(111)	2.8	0.49	1.4	1.00
(210)	2.8	0.49	1.2	1.00
(311)	2.8	0.49	1.2	1.00
(311) (4N)	3.5	0.50	5.0	1.02
C. Step measurements after Frumkin correction				
(110)	1.2	0.51	1.2	1.00
	1.0	0.52	1.2	1.00
(100)	0.65	0.51	0.9	1.00
(111)	0.55	0.50	0.8	1.00
D. Sweep measurements after Frumkin correction				
(110)	0.75	0.50	0.6	1.00
(100)	0.5	0.50	0.7	1.00
(111)	0.7	0.50	2.0	1.00

$\theta_H \gg 0.5$ or mechanism A with $\theta_H \ll 0.5$. (Mechanism B with $\theta_H \ll 0.5$ is excluded, because it would never lead to an increase of θ_H going to low current densities). We conclude that the mechanistic construction could be as follows:

(a) In the more negative potential region the proton reduction proceeds by R1 followed by R2, with either of them rate-determining.

(b) At less negative potentials the proton reduction involves fast proceeding of R1, followed by either R2 or R3 as the rate-determining step. In view of the value found for ν'_{H^+} (see section IV.2), R3 would be more probable than R2.

As argued before, this conclusion is based upon the assumption that stationary state behaviour exists, at least on the dc time scale (corresponding to electrolysis times of 4 s). On the ac time scale it is sufficient to assume that the low frequency limit of eqn. (10) applies, so that the experimentally obtained charge transfer resistance obeys eqn. (11) and thus eqn. (9), as is found in Fig. 6. It is worth noting that the impedance data give no evidence of any adsorption capacitance, which, if it were present, would presumably be a function of potential. However, it is quite probable that its value is extremely small in our case, since it is reported that the maximum coverage Γ_m of hydrogen adsorption, and thus C_H in eqn. (10), should be extremely small, as would be expected from the absence of detectable hydrogen adsorption on the voltammograms.

It is difficult to compare our reasonings with the rather inconsistent evidence present in the literature. In the review given by Kuhn and Byrne [7] it can be seen that usually only one Tafel slope is reported, but a variety of values between 0.12 V ($\alpha = 0.5$) to 0.03 V ($\alpha = 2$) was found. Kuhn and Byrne themselves, in fact, proposed the same mechanistic scheme as we suggested above on the basis of the observation of two Tafel slopes, $\alpha \approx 0.5$ and $\alpha \approx 2$, with a sharp transition in between. This must mean that in their case always $\theta_H \ll 0.5$. However, the two exchange current densities that can be derived from their results are $i_0 = 40 \times 10^{-6}$ A cm^{-2} (high current densities where $\alpha = 0.5$) and $i_0 = 3 \times 10^{-6}$ A cm^{-2} (low current densities where $\alpha = 2$). These values are much higher than can be calculated from our data: $i_0 = 5.8 \times 10^{-6}$ A cm^{-2} (at high current densities where $\alpha = 0.5$) and $i_0 = 0.21 \times 10^{-6}$ A cm^{-2} (at low current densities where $\alpha = 1$). The former value agrees well with the values selected in ref. 13 (Table 2.1.1) as "reliable" ones. It must be concluded therefore that Kuhn and Byrne have worked with much more reactive gold surfaces. Moreover, a closer inspection of their results at three different concentrations (0.01, 0.1 and 1 M H_2SO_4) reveals that no single reaction order with respect to c_{H^+} for j_F at fixed $E - E^\circ$ can be defined and at low current densities it is certainly not equal to $\nu_{H^+} = 2$ as it should be.

It seems not strictly necessary to relate our experimental findings to the classical mechanistic scheme as given in Section (III.1) by the reaction R1, R2 and/or R3. An alternative scheme could be the following:

$$H^+(H_2C)_h + e^- \underset{k_{-1}}{\overset{k_1}{\rightleftarrows}} h\,H_2O + H_{ad} \qquad (R1')$$

$$H_{ad} + \text{site} \rightarrow H_{site} \qquad (R2')$$

$$H_{ad} + H_{site} \rightarrow H_2 + site \qquad (R3')$$

The idea behind this scheme is to suppose the presence of "sites" (presumably foreign atoms) on the surface where H-atoms are adsorbed more strongly than at the gold atoms and that the recombination reaction proceeds at these sites preferably. If reaction R2′ proceeds so fast that all sites are continuously occupied, the recombination process (R2′ + R3′) becomes pseudo-first order in c_H (the interfacial concentration of the intermediate H_{ad}), as we will have $v_2 = v_3 = k_3' c_H$, with k'_3 being proportional to the density of sites. In the stationary state $v_1 = v_2 + v_3 = 2v_3$, and consequently the overall forward rate constant will obey the expression

$$\frac{1}{k_f} = \frac{1}{k_1} + \frac{K_1}{2k'_3} = \frac{\exp(\alpha_1 \phi)}{k_{s_1}} + \frac{\exp(\phi)}{2k'_3 \exp[(F/RT)(E^\circ_1 - E^\circ)]} \qquad (13)$$

where $k_{s_1} = k_1(E = E^\circ)$ and E°_1 is the standard potential of the discharge reaction. The potential dependence of k_f in eqn. (13) is the same as that in the empirical eqn. (12) if α_1 equals 0.5. So, the scheme R1′, R2′, R3′ conforms to our experimental results. Although at present a definite proof is not possible, we think that this mechanism is quite probable in cases where the electrode surface has an extremely low density of sites.

In contrast with the classical schemes, the alternative involves both "strongly adsorbed" and "weakly adsorbed" hydrogen atoms, the latter produced at any point of the surface. This idea bears a resemblance to what is suggested to be the state of photo-electrochemically generated H-atoms [30,31]. However, the results for the photogenerated atomic hydrogen appear to depend on the crystallographic orientation of the surface of the gold electrode [32] so another mechanism might be operative in this case. On the other hand, our results could equally well be explained assuming the idea that the proton discharge, reaction R1, is rate determining over the whole potential range of our measurements, but only changes from the "ordinary" behaviour to the behaviour corresponding to "barrierless discharge" [29,30,33–35]. At present it seems that a logical decision between various models is still hard to make. Probably a well planned study of the reaction at gold electrodes with a deliberately modified number of adsorption sites is quite valuable for this purpose.

(V.3) Effects of crystallographic orientation

In a recent compilation of data on the proton reduction [13] it is concluded that exchange current densities are not significantly different at different crystal faces of either V, Ni, Cu, Mo, W or Pt.

In view of Fig. 7 and the data in Table 3, sections A and B, the same conclusion seems to apply for gold, although some plane-specificity is seen in the results of the potential step method. However, it is known that the potential of zero charge strongly depends on the crystallographic orientation and therefore a more proper comparison can be made after accounting for the influence of the double-layer structure, i.e. the Frumkin correction. For this purpose we estimated the potential,

ϕ_2, in the outer Helmholtz plane from the integrated double-layer capacities from Fig. 3, using the following values of the pzc: for the (110) plane −0.06 V vs. SSCE, for the (100) plane +0.10 V vs. SSCE, for the (111) plane +0.20 V vs. SSCE. These values were obtained from the minima in the capacity–potential curves measured in 0.01 *M* $HClO_4$ at our own electrodes and compare satisfactorily with values of the pzc obtained in $HClO_4$ solutions for the (100) face [18] and the (111) face [36]. Absence of specific adsorption of H^+ and ClO_4^- was assumed [18].

So-called Frumkin corrected plots were obtained from the results of the potential step measurements by plotting $\ln(k_f) + (F/RT)\phi_2$ vs. $E - \phi_2$, leading to Fig. 8. The conclusion is that the differences in the kinetics between the three crystal faces are of the same order of magnitude as in the non-corrected plots of Fig. 7. The conformity with eqn. (12) is maintained as follows from the data in Table 3, section C. Note that both the corrected L_1 value and the corrected L_2 value appear to depend (slightly) on the crystallographic orientation in the order (111) < (100) < (110). However, a different trend is observed in the results from the potential sweep measurements given in Table 3, section D.

At present it seems impossible to think of an entirely satisfactory interpretation of this result. It is well-known that the rate of proton reduction strongly depends on the

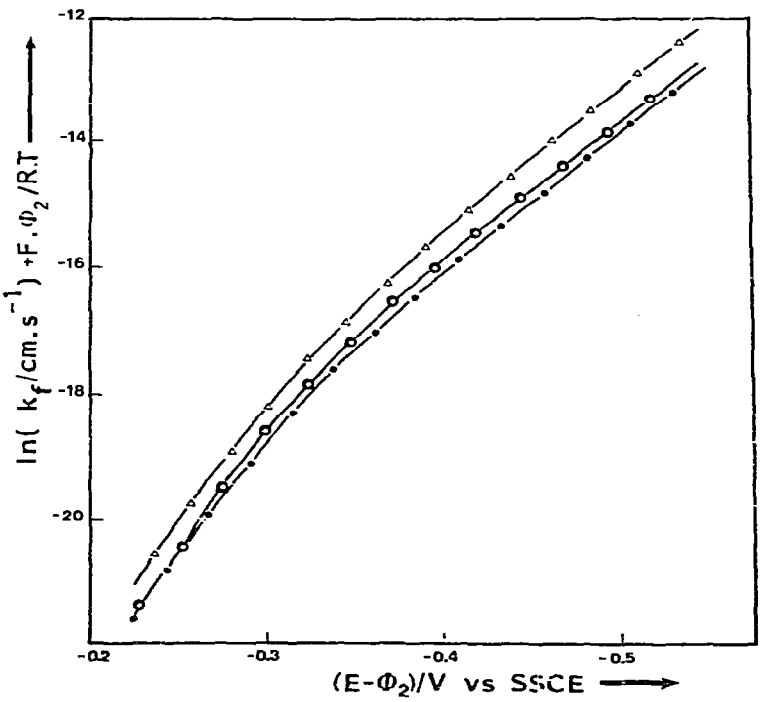

Fig. 8. Frumkin corrected plots, ln $k_f + (F/RT)\phi_2$ vs. $E - \phi_2$ for 1 *M* perchloric acid. (△) (110), (○) (100), (●) (111).

nature of the electrode metal and this has frequently been discussed in the literature [9,11,13,14,34]. It should be concluded that the well-known (empirical) correlation with the electronic work function (ϕ_e) does not apply if faces of the same metal but with different crystallographic orientation are compared. For example, from Table 3A we calculate the following exchange current densities (i_0):

(110): 3.7×10^{-6} and 1.0×10^{-7} A cm^{-2}

(100): 3.4×10^{-6} and 0.7×10^{-7} A cm^{-2}

(111): 1.75×10^{-6} and 0.8×10^{-7} A cm^{-2}

(the first column applying to the more negative part, and the second to the less negative part of the potential region studied). When the parallelism between the pzc and the electronic work function is accepted [37], the difference in electronic work function between Au(110) and Au(111) amounts to $\Delta\phi_e \approx 0.3$ eV, so we find $\Delta \log i_0/\Delta\phi_e \approx -1.1$, according to the first column. This is quite different from the value corresponding to exchange currents and work functions at different electrode metals, viz. $\Delta \log i_0/\Delta\phi_e \approx 7$, as has been calculated by Trasatti in his well-documented review [14]. Recently the weak variation of activity for hydrogen evolution with crystal face orientation was discussed and some possible explanations were given [15].

It has also been argued [9,10] that the primary property for a correlation should be the Gibbs energy of adsorption of atomic hydrogen. However, it is not known whether this quantity could be more or less dependent on the orientation of the lattice plane in the case of gold.

A correlation of the rate of the discharge reaction with the adsorption enthalpy will be irrelevant if the mechanism discussed in Section (IV.3.2) holds. In this case it is more feasible to think of an additional specific double-layer effect, e.g. inherent to a difference in the electric field strength in the inner layer. In view of this it could be interesting to obtain more information about the degree of the hydration of H^+ and the way the hydration sheath is removed before or after electron transfer. Also, it should be investigated whether it is correct to assume the absence of any (perhaps orientation dependent) specific adsorption of the perchlorate ion. It is reasonable to believe the density of active sites to depend on crystallographic orientation, which could, via k'_3 in eqn. (13), explain the variations of L_2 in Table 3.

With a view to the distinct difference of the rate of R1 obtained at 4 N and 5 N quality of gold we should be aware that dependence of the kinetics on crystal face orientation could originate from orientation-dependent surface excesses of impurities. Experiments with intentionally contaminated electrode surfaces and intentionally contaminated bulk electrode material would be most elucidative on this point.

ACKNOWLEDGEMENTS

The authors wish to express their gratitude to Mr. A. van den Eeden and Mr. J.W. Deneer for valuable discussions and technical assistance, to the referee of this paper

for his detailed comments and valuable suggestions and to Dr. R. Parsons for his critical, but helpful assistance in preparing the final manuscript.

REFERENCES

1 D. Dickertmann, F.D. Koppitz and J.W. Schultze, Electrochim. Acta, 21 (1976) 967.
2 A. Hamelin and A. Katayama, J. Electroanal. Chem., 117 (1981) 221.
3 A. Hamelin, T. Vitanov, E. Sevastyanov and A. Popov, J. Electroanal. Chem., 145 (1983) 225.
4 M.W. Breiter, J. Electroanal. Chem., 8 (1964) 230.
5 S. Gilman, Electrochim. Acta, 9 (1964) 1025.
6 M. Sluyters-Rehbach and J.H. Sluyters in J.O'M Bockris and E. Yeager (Eds.), Comprehensive Treatise on Electrochemistry, Vol. 9, Ch. 4, in press.
7 A.T. Kuhn and M. Byrne, Electrochim. Acta, 16 (1971) 391.
8 T. Sasaki and K. Matsuda, J. Res. Inst. Catal. Hokkaido Univ., 21 (1973) 157; 29 (1981) 113.
9 R. Parsons, Trans. Faraday Soc., 54 (1958) 1053.
10 H. Gerischer and W. Mehl, Z. Elektrochem., 59 (1959) 1049.
11 A.N. Frumkin in P. Delahay (Ed.), Advances in Electrochemistry and Electrochemical Engineering, Vol. 1, 1961, pp. 65–121; Vol. 3, 1963, pp. 287–391, Interscience, New York.
12 E. Gileadi and B.E. Conway in J.O'M Bockris (Ed.), Modern Aspects of Electrochemistry, Vol. 3, Butterworths, London, 1964, pp. 381–397.
13 A.J. Appleby, M. Chemla, H. Kita and G. Bronoël in A.J. Bard (Ed.), Encyclopedia of Electrochemistry of the Elements, Vol. IXa, Marcel Dekker, New York and Basel, 1982, pp. 413–556 (and references cited therein).
14 S. Trasatti, J. Electroanal. Chem., 39 (1972) 163.
15 S. Trasatti, Proc. Symp. "The Chemistry of Electrocatalysis", San Francisco, May 1983, The Electrochemical Society, Pennington, 1983, Ext. Abstr. 83-1, p. 1038.
16 L. Bicelli and M.R. Graziano, Rend. Ist. Lomb. Accad. Sci. Lett., A96 (1962) 98.
17 J.K. MacKenzie, A.J. Moore and J. Nicholas, J. Phys. Chem. Solids, 23 (1962) 185.
18 A. Hamelin and A. Lelan, C.R. Acad. Sci. Ser. B, 295 (1982) 161.
19 J. Clavilier, R. Faure, G. Guinet and R. Durand, J. Electroanal. Chem., 107 (1980) 205.
20 C.P.M. Bongenaar, M. Sluyters-Rehbach and J.H. Sluyters, J. Electroanal. Chem., 109 (1980) 23.
21 J. Clavilier, C.R. Acad. Sci. Ser. C, 263 (1966) 191.
22 A.N. Frumkin, P. Dolin and B. Ershler, Acta Physicochim. USSR, 13 (1940) 779.
23 B.E. Conway and M. Salomon, Electrochim. Acta, 9 (1964) 1599.
24 A.J. Bard and L.R. Faulkner, Electrochemical Methods, John Wiley and Sons, New York, 1980, p. 166.
25 G.J. Brug, A.L.G. van den Eeden, M. Sluyters-Rehbach and J.H. Sluyters, J. Electroanal. Chem., 176 (1984) 275.
26 M. Sotto, J. Electroanal. Chem., 69 (1976) 229.
27 D. Dickertmann, J.W. Schultze and K.J. Vetter, J. Electroanal. Chem., 55 (1974) 429.
28 G.M. Schmid, Electrochim. Acta, 12 (1967) 449.
29 L.I. Krishtalik, J. Electroanal. Chem., 100 (1980) 547.
30 L.I. Krishtalik, J. Electroanal. Chem., 130 (1981) 9.
31 R. Parsons, G. Picq and P. Vennereau, J. Electroanal. Chem., 146 (1983) 123.
32 A. Hamelin, G. Picq and P. Vennereau, J. Electroanal. Chem., 148 (1983) 61.
33 L.I. Krishtalik, Electrochim. Acta, 13 (1968) 1045.
34 L.I. Krishtalik in P. Delahay (Ed.), Advances in Electrochemistry and Electrochemical Engineering, Vol. 7, Interscience, New York, 1970, p. 283.
35 R.R. Dogonadze in N.S. Hush (Ed.), Reactions of Molecules at Electrodes, Wiley-Interscience, London, 1971, p. 135.
36 A. Hamelin and Z. Borkowska, unpublished results.
37 J. Lecoeur, J. Andro and R. Parsons, Surf. Sci., 114 (1982) 320.